INSTITUTE OF PHYSICS PUBLISHING and INTERNATIONAL ATOMIC ENERGY AGENCY NUCLEAR FUSION

Nucl. Fusion **43** (2003) 262–267 PII: S0029-5515(03)60741-6

MHD stability analysis of type II ELMs in ASDEX Upgrade

S. Saarelma[1], S. Günter[2], L.D. Horton[2] and ASDEX Upgrade Team[2]

[1] Helsinki University of Technology, Euratom-TEKES Association, FIN-02015 HUT, Finland
[2] Max-Planck-Institut für Plasmaphysik, EURATOM Association, Boltzmannstr. 2, D-85748 Garching, Germany

E-mail: samuli.saarelma@hut.fi

Received 10 October 2002, accepted for publication 3 March 2003
Published 27 March 2003
Online at stacks.iop.org/NF/43/262

Abstract
We investigated the differences between type I and type II edge localized modes (ELMs) in ASDEX Upgrade using the MHD stability analysis. When plasma conditions are changed from typical type I ELMy conditions to type II ELMy conditions, the character of the edge instabilities change. With increased triangularity and edge safety factor, the low-n peeling–ballooning mode becomes more stable and more localized to the edge region. We find the same mode localization effect in almost double null configuration. When the plasma density is increased, the access to the second stability of the high-n ballooning modes is closed. The changes in the stability properties give a qualitative explanation to the observed small amplitude of the type II ELMs.

PACS numbers: 52.35.Py

1. Introduction

For a tokamak reactor operating in the high confinement mode (H-mode), such as ITER, high power load on divertor plates can cause unacceptable erosion and should therefore be avoided. H-mode plasmas are usually characterized by edge-localized modes (ELMs) that release plasma particles and energy from inside the separatrix into the scrape-off-layer (SOL) in short bursts. From the SOL the energy is transported to the divertor plates along field lines. Since the phenomenon is fast ($t < 1$ ms), the high power load on targets during an ELM poses a threat to the reliable quasi-steady state operation of a tokamak. However, while detrimental to the divertor plates, ELMs can help to control the plasma density and impurity accumulation. Therefore, the control of the ELM behaviour is of great importance for a tokamak reactor.

The type I or 'giant' ELMs, observed in most H-mode plasmas, are large in amplitude, and thus the most detrimental to the divertor plates. In ITER the type I ELM energy may exceed the threshold for divertor target ablation by a factor of 5 [1].

The type II or 'grassy' ELMs show potential to operate a tokamak with good confinement and efficient impurity exhaust without damaging the divertor plates. The energy lost in a single type II ELM is significantly lower than in a type I ELM. Respectively, the ELM frequency of type II ELMs is usually higher than that of type I ELMs for similar heating and collisionality.

The type III ELMs are also small in amplitude. However, the plasma confinement in type III ELMy plasma is poor. Therefore, combining the type III ELMs and high β is difficult and, thus, they are not considered in this paper.

The fundamental mechanisms behind the ELM phenomenon is not known. Several possible explanations have been given [2]. The model presented for type I ELMs by Connor *et al* [3] and expanded by Snyder *et al* [4] for other ELM types is used here as a working model. In this model, the type I ELMs are triggered by coupled peeling–ballooning mode MHD instabilities. After an ELM crash, the plasma edge pressure gradient starts recovering until it reaches the high-n ballooning mode boundary. Then, on a slower (resistive) timescale, the edge bootstrap current builds up. The bootstrap current destabilizes the peeling–ballooning mode and causes an ELM crash.

In an earlier study [5], the Connor model was studied by carrying out a stability analysis for type I ELMs in ASDEX Upgrade. It was found that the edge pressure gradient is indeed limited by the ballooning mode between ELMs, when the edge current is low. When the bootstrap current builds up, the plasma can access the 2nd stable region. The analysis also showed that the increasing bootstrap current destabilizes the low-n ($n \approx 3$–4) peeling–ballooning mode. In the stability analysis, the mode numbers of the unstable modes agreed with the experimental values. Although the linear stability analysis naturally cannot directly predict the repetition frequency of

the ELMs, the stability analysis results were able to explain the observed type I ELM precursors.

In this paper, using the same model, we now expand the stability analysis to type II ELMs in ASDEX Upgrade. Experimentally, it has been observed that when the plasma conditions are changed, the ELM behaviour also changes. In particular the change from type I to type II ELMs is observed as triangularity, edge safety factor and density are increased and the plasma is moved close to double null configuration. First the pure type I ELMs change to mixed ELMs with both large and small amplitude ELMs and finally to pure type II ELMs [6]. In addition to the direct changes in the equilibrium, like shaping and increasing the edge q, there are also indirect changes. When plasma approaches the double null configuration, the local shear increases in the region close to the second x-point. The increased edge density combined with constant pressure leads to increased collisionality that decreases the bootstrap current. Due to the changes in the equilibrium, the character of the MHD instabilities in the edge plasma change as well. The changes in the edge stability properties can be used to explain the changes in the ELM behaviour.

2. Equilibrium reconstruction

In the equilibrium reconstruction, plasma pressure and poloidal current are needed to solve the Grad–Shafranov equation. The pressure profile can be obtained from the experiment, but the current profile is not usually measured directly. However, the edge current plays an important role in the stability of the edge plasma. Therefore, in order to draw any conclusion from the modelling, the edge current in the reconstructed equilibrium must have the same response to the plasma condition changes as the actual plasma current. The accuracy of the core current profile is not equally critical, since it has little effect on the very localized instabilities at the edge.

In the H-mode pedestal region, the bootstrap current dominates the inductively driven current because of the steep pressure gradient. The bootstrap current was included in the equilibrium calculation using an analytical formula for the flux averaged parallel bootstrap current $\langle \boldsymbol{j} \cdot \boldsymbol{B} \rangle / (\mu_0 J)$ given by Sauter *et al* [7]. In the core, we assume the inductively driven current to dominate, and choose its profile to fit to the available core q-profile information ($q_{\mathrm{axis}} \approx 1.1$). The total plasma current is kept at the experimental value. Using these boundary conditions together with the measured density and temperature, it is possible to create self-consistent equilibria for stability analysis. The self-consistent bootstrap current equilibrium reconstruction has an additional advantage allowing realistic stability studies by artificially varying density and temperature profiles. Furthermore, the current diffusion to the edge region between the ELMs is relatively slow compared to the return of the H-mode pedestal. It is possible to simulate this by including less than 100% of the bootstrap current in the equilibrium reconstruction.

We take the density and temperature profiles and the plasma shape for the studied equilibria from the experiment (ASDEX Upgrade shot no 11991 at 2.0 s, $I = 1.0$ MA, $B_{\mathrm{T}} = 2.0$ T, the profiles shown in figure 1). The error in the profiles is 10%. The profile for the effective charge number (Z_{eff}) is assumed flat with a value of 1.2.

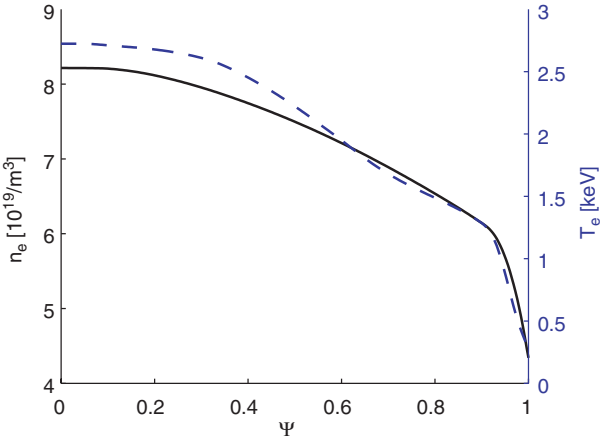

Figure 1. The temperature (- - - -) and density (——) profiles used in the equilibrium reconstruction as a function of the poloidal flux. $T_{\mathrm{e}} = T_{\mathrm{i}}$ is assumed.

In the stability analysis, we vary the plasma parameters to see the effect of each factor on the stability. In addition, we analyse two shots (nos 15865 and 15863, both with $I = 0.8$ MA, $B_{\mathrm{T}} = 2.0$ T) with almost identical plasma profiles, but slightly different shapes. These shots are chosen because one (no 15865) displayed type I ELMs and the other (no 15863) type II ELMs.

3. The type II ELM condition effects on the ELM model

It has been shown that the the stability analysis of ASDEX Upgrade type I ELMs gives results consistent with Connor's model for ELM triggering [5]. Here, the stability analysis is extended to conditions where smaller type II ELMs are observed. In ASDEX Upgrade, the requirements for achieving high frequency, low amplitude type II ELMs are high triangularity, high q_{95}, almost double null configuration, and sufficiently high density [6]. Also in JT-60U high triangularity and edge safety factor are found to suppress the giant ELMs [8]. We include all these factors in the stability analysis and study each of them independently using the ideal MHD stability code GATO [9] for peeling–ballooning modes with low and intermediate toroidal mode number ($n \leqslant 8$). Most of the analyses are done for $n = 3$ because in the experiment, $n \approx 3$ and 4 precursor activity was observed for both type I and type II ELMs [6,10]. The IDBALL code is used for $n = \infty$ ballooning modes.

In the calculations, the conductive wall is assumed to be far from the plasma. Since the modes have very localized structure, a more realistic treatment of the wall structures would have little effect on the results.

3.1. Triangularity and edge safety factor

To investigate the effect of the triangularity and edge safety factor on the edge stability, we take the earlier type I ELM study as a starting point. We modify the equilibrium by changing the plasma shape and q-profile while keeping the density and temperature profiles unchanged. Type I ELMy plasma is characterized by low triangularity ($\delta < 0.3$) and low

safety factor at the edge ($q_{95} < 4.5$). To simulate type II ELMy plasma conditions we increase both the triangularity and q_{95} ($\delta = 0.45$, $q_{95} = 5.0$). The triangularity is increased by shaping the plasma using the poloidal coils and the q-value by increasing the toroidal magnetic field. The stability analysis shows that when the triangularity and q_{95} are increased, the edge pressure gradient and, consequently, also the bootstrap current at the edge can be increased 30% higher before plasma becomes low-n peeling–ballooning mode unstable. The result agrees with the stability calculations for $n = 5$ mode for triangularity scans in DIII-D [11] as well as low-n mode stability analyses in JET [12] and JT-60U [13]. The higher stability limit also agrees qualitatively with the observed high pedestal pressure in ASDEX Upgrade in high triangularity discharges [14].

In addition to the stabilizing effect, the eigenfunction of the unstable mode becomes narrower. This is shown in figure 2 for $n = 3$. Lower mode numbers ($n = 1$, $n = 2$) remain stable even with increased edge pressure gradient. It should be noted here that neither of the factors (δ or q_{95}) alone is sufficient to make the eigenfunction of the instability narrow, but both are required. On the other hand, increasing triangularity improves the plasma stability against low-n peeling–ballooning modes even when q_{95} is kept fixed.

The triangularity has very little effect on the ballooning stability except for the very edge (normalized poloidal flux $\psi > 0.98$). If the density is kept low, both the plasma with high triangularity ($\delta = 0.45$) and low triangularity ($\delta = 0.15$) have second stability access in the steepest pressure gradient region ($0.94 < \psi < 0.98$) with the experimental density and temperature and self-consistent bootstrap current. Only in the very edge ($\psi > 0.98$) does the pressure gradient of the low triangularity plasma become limited while the high triangularity plasma stays in the second stable region.

The normalized pressure gradient α increases with the increasing q because $\alpha \sim q^2$. However, the second stability access depends only on the shear (sufficiently low shear opens the access), and if the second stability access is open, α is not limited by the $n = \infty$ ballooning mode at all. Therefore, varying q_{95} has no effect on the second stability access of the edge ballooning modes as long as the edge shear remains unchanged in such a variation.

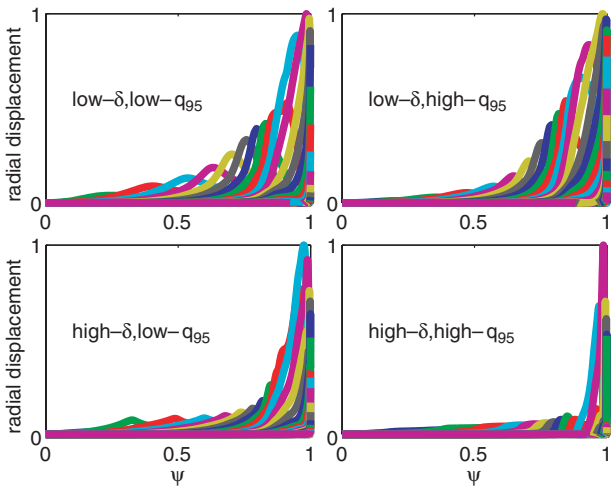

Figure 2. Fourier analysis of the eigenfunctions of the radial displacement for the $n = 3$ peeling–ballooning mode for different q_{95}–δ combinations. Each curve represents the eigenfunction of a single poloidal mode number. Low-$q_{95} = 4.3$, high-$q_{95} = 5.0$, low-$\delta = 0.15$, high-$\delta = 0.45$.

Assuming that the instability removes edge plasma in a region of a width proportional to its eigenfunction width, increasing triangularity and edge safety factor would imply reduced loss of plasma during an ELM crash. However, since the stability is also improved, higher edge pressure gradient and bootstrap current is required to destabilize the low-n peeling–ballooning mode. If the pressure gradient is not limited by the $n = \infty$ ballooning mode, the triggered ELM crash can happen at a higher value of pedestal pressure. This could actually lead to a larger loss of plasma, if the low-n peeling–ballooning mode is indeed the main cause for the loss of plasma during an ELM. However, if the pressure gradient becomes limited by the ballooning mode, while the stability boundary for low-n modes remains high, the low-n modes will never become unstable, and the only unstable modes are those with higher n. They have narrower mode width than the low-n modes and the resulting ELM would be small. Therefore, in order to achieve small plasma losses, the changes in low-n peeling–ballooning mode stability must be accompanied by the closing of the second stability access for $n = \infty$ ballooning modes, for instance, by increased shear.

It must be noted that because of the geometry of the device, the position of the shaping coils in particular, increasing triangularity by using shaping coils necessarily moves the second x-point closer to the separatrix. Therefore, the triangularity effect on the stability can be partly due to the double null effect that we will also show to have similar effect on the stability.

3.2. Density

The density has an indirect effect on the edge stability through the bootstrap current. If the pedestal pressure is assumed fixed, increasing density lowers temperature. This in turn increases the plasma collisionality at the edge and, thus, reduces the bootstrap current without lowering the pressure gradient. This has a stabilizing effect on the low-n peeling–ballooning mode. The stabilizing effect of the high density is shown in figure 3, where the pressure is kept fixed and temperature and density are varied for two different plasma shapes. The stabilizing effect of increased density on the low-n peeling–ballooning modes applies both to single and double null configurations.

The increasing density has the opposite effect on the $n = \infty$ ballooning stability. In figure 4, the ballooning stability boundary for α ($=2Rq^2(\mathrm{d}p/\mathrm{d}r)/B^2$) is plotted for two different densities. Again, we keep the pressure at the experimental value (ASDEX Upgrade shot no 15863) and decrease the temperature as the density is increased. The increased density-temperature ratio increases the collisionality (from $\nu_{*e} \approx 2.8$ at the top of the pedestal, to $\nu_{*e} \approx 5.5$) and reduces the bootstrap current near the edge. In the low density case, the second stability access is open in the entire pedestal region, but in the high density case, the access is closed. It must be noted that in order to close the second stability access in the entire pedestal region, the density is increased by 30%. However, even a more modest (10%) density increase can make

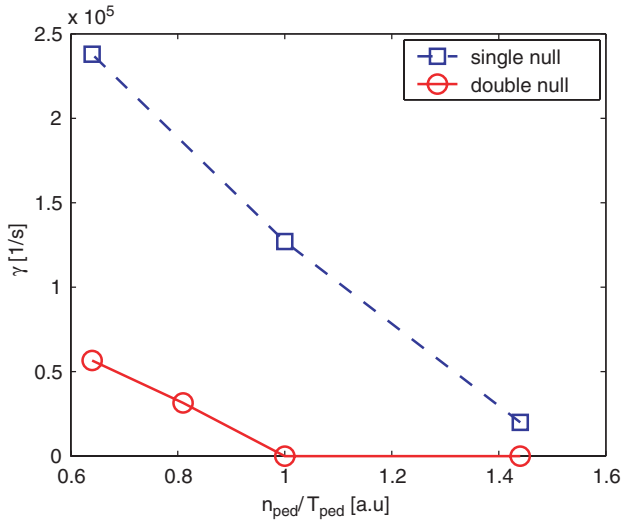

Figure 3. The $n = 3$ peeling–ballooning mode growth rate as a function of the pedestal density-to-temperature ratio. The value 1 is the experimental value.

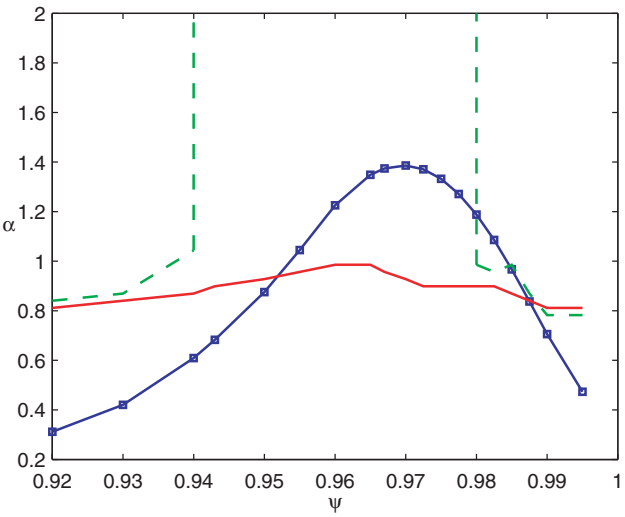

Figure 4. The experimental α in the pedestal region (——■——) together with $n = \infty$ ballooning mode stability boundary at the plasma edge for high ($\bar{n} = 1.1 \times 10^{20}\,\mathrm{m}^{-3}$, ——) and low ($\bar{n} = 0.9 \times 10^{20}\,\mathrm{m}^{-3}$, - - - -) densities. The open gap from $\psi = 0.93$ to 0.987 for the low density case represents access to second stability.

the second stable region considerably narrower than in the low density case. In this case, the second stability access is achieved only between $\psi = 0.95$ and 0.96. Except for this narrow gap, the access is closed in the pedestal region.

The closing of the second stability access by the high collisionality means that in high density plasmas the edge pressure gradient becomes limited by the ballooning mode. For low density plasmas, the pedestal pressure gradient is not limited by MHD instabilities until the bootstrap current increases sufficiently to destabilize the low-n peeling–ballooning mode. As shown in the previous section, in type II ELM conditions (high δ and q_{95}), the low-n stability boundary allows a higher value for the pressure gradient. If the pressure gradient is now limited by the high ballooning mode due to the increased collisionality, it is possible that the wide low-n modes are entirely avoided, and the ELM is triggered only by an intermediate-n peeling–ballooning mode with much narrower radial extent. The resulting ELM then leads to a smaller loss of plasma.

3.3. *Closeness to double null*

To investigate the significance of the closeness to the double null we analyse two ASDEX Upgrade plasmas (nos 15863 and 15865) with almost identical density and temperature profiles and $\delta = 0.42$, $q_{95} = 4.2$, but one with slightly closer to double null. These shots are chosen because one of them (no 15865) has mixed type I and type II ELMs and the other one (no 15863) pure type II ELMs. We complete the analysis with an artificial plasma with the same profiles, but in a full double null configuration. We determine the stability boundary for the low- to intermediate-n modes by scaling the edge temperature gradient and, thus, the pressure gradient and indirectly also the edge bootstrap current. Since GATO can use only closed field line configurations, plasma boundary is moved $\psi = 2 \times 10^{-4}$ inside the separatrix to avoid the x-point. The part that is cut away is very narrow. Therefore, the high increased shears effect produced by the second x-point is retained.

We find the double null configuration to have a stabilizing effect on the low-n peeling–ballooning modes. The second x-point creates a strong magnetic shear in its vicinity (just like the first x-point). The increased shear eliminates the peeling–ballooning mode near the x-points as can be seen in figure 5 for an $n = 3$ mode. Figure 6 shows the growth rates for the $n = 3$ mode as a function of the maximum pressure gradient in the pedestal region for the different configurations. The plasma with type II ELMs has lower growth rate than the type I ELMy plasma. The growth rate for a double null plasma is even lower. However, as the mode number increases, the growth rate increases in both plasmas. The higher the mode number, the smaller the pressure gradient required to destabilize it. On the other hand, the mode width decreases with the increasing mode number. Consequently, the higher modes can directly affect only a very narrow part of the plasma.

The double null configuration also makes the low- to intermediate-n peeling–ballooning mode strongly localized at the edge. The localization effect is prevalent irrespective of the mode number. Even a small shift of the plasma towards the upper x-point can lead to a significant change in the eigenfunction width. This is shown for an intermediate-n mode ($n = 8$) in figure 7. The vertical position of type I and type II ELMy plasmas differ only by a few millimetres at the midplane. On the top of the plasma, the type II ELMy plasma is 8 cm closer to the second x-point.

The $n = \infty$ ballooning stability is also affected by the double null. The shear at the low field side is increased only little by the second x-point, but the most important shaping effect is the slight widening of the second stability access. However, when the density increases, the second stability access closes also for the double null configuration just as in the single null plasma. The density increase needed to close the second stability access is increased by 10% the double null configuration.

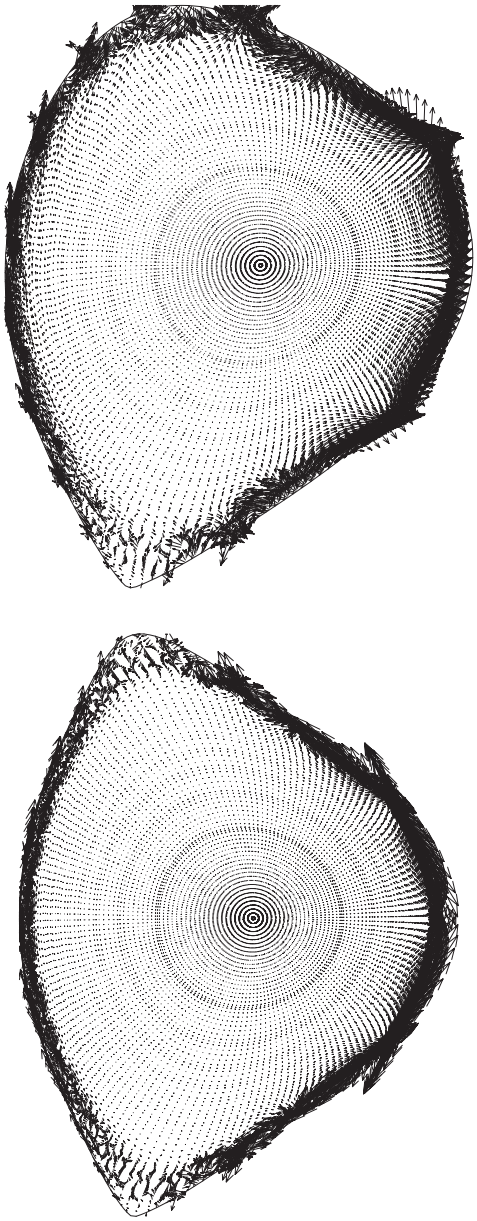

Figure 5. The $n = 3$ peeling–ballooning mode structure for single and double null plasmas. Both upper and lower x-point eliminate the mode from their vicinity.

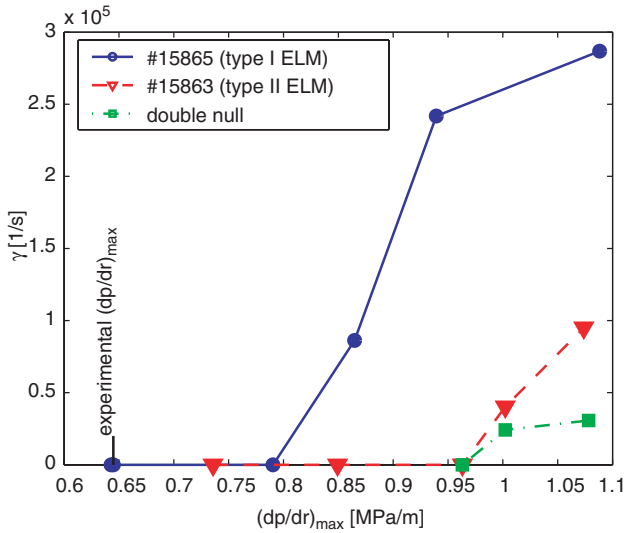

Figure 6. The $n = 3$ peeling–ballooning mode growth rate as a function of the edge pressure gradient for plasmas with type I (no 15865) ELMs, type II (no 15863) ELMs and for a double null configuration.

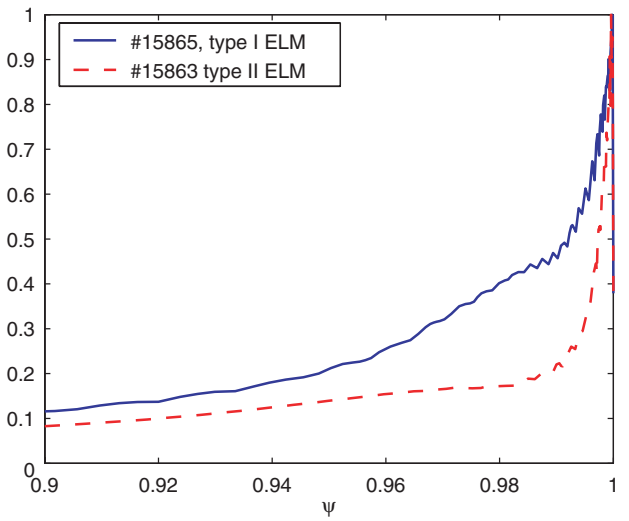

Figure 7. The $n = 8$ peeling–ballooning mode radial envelope (the normalized sum of Fourier components of the $\xi \cdot \nabla\psi/|\nabla\psi|$) for type I (no 15865) and type II (no 15863) ELMy plasmas. The pedestal top is at $\psi = 0.94$. Note that both modes are narrower than the pedestal.

4. Conclusions

The above stability analysis allows for a qualitative understanding of how the experimentally observed critical parameters affect the ELM behaviour. We showed how the stability properties of the edge plasma change, when the plasma conditions are changed from those of type I ELMs to those of type II ELMs. The most significant change is the strong localization of the peeling–ballooning mode with high triangularity, increased edge safety factor and moving plasma closer to the second x-point. This effect applies to all investigated mode numbers ($n = 3$–8). The even lower mode numbers ($n = 1$ and 2) are not affected, since they are stable in all cases. The stability boundary (as a function of the pressure gradient) of the $n = 3$ mode is also increased in type II ELMy conditions. On the other hand, the instabilities with an intermediate mode number (e.g. $n = 8$) were not stabilized, but only the mode width became narrower in type II plasmas.

The non-linear development of the unstable mode was not investigated, but we can assume that the effect that an instability has on the plasma depends on its mode structure. A radially extended mode should expel more plasma than a narrow one. With this assumption the observed differences between type I and type II ELMs can be explained using the stability analysis results. Both type I and type II ELMy plasma equilibria with self-consistent bootstrap current become first unstable to an intermediate-n peeling–ballooning mode. The instability has a narrow eigenfunction and affects only the

very edge of the plasma ($\psi > 0.98$). However, for type I ELMy plasmas, the wide (radial extent $0.7 < \psi < 1.0$) low-n mode stability boundary is close to the stability boundary of the intermediate-n modes. Thus, the low-n modes could become destabilized as the very narrow mode removes plasma from the edge and the pressure gradient becomes steeper. The wide low-n peeling–ballooning mode can then remove significant amount of plasma from the edge. On the other hand, the type II ELMy plasmas are more stable against the low-n modes. Furthermore, for type II ELMy plasmas the mode width of the intermediate-n mode is narrower and, thus, the effect on the edge profiles is smaller. The high density in type II ELMy plasmas keeps the bootstrap current low in the pedestal region. This closes the second stability access for ballooning modes and keeps the pressure gradient limited. Consequently, type II ELMy plasmas do not become unstable for low-n peeling–ballooning modes that have a wide radial structure. The pressure gradient is relaxed before the bootstrap current can destabilize these modes. In an ELM crash triggered by a narrow intermediate-n peeling–ballooning mode only a very narrow part of the edge plasma is lost and the resulting ELM is small in amplitude. The improved stability against the low-n modes and the narrow mode structure of the intermediate-n modes agrees with the qualitative type II ELM model presented in [4].

Also the difference in repetition frequencies can be explained by differences in plasma conditions. First, since the type II ELM is small, less current is lost at the edge during an ELM crash. Additionally, the higher resistivity in type II ELMy plasmas (due to low temperature and high density at the pedestal) increases the current diffusion in the edge region making the current recovery after an ELM faster. When the bootstrap current has recovered from the previous ELM crash, the stability limit is reached again and another ELM is triggered. The entire ELM cycle becomes faster as the current diffusion increases and the ELMs occur more frequently.

The integrated effect of the changes in stability properties and speed of the current diffusion is thus that the type II ELMs are smaller and more frequent than type I ELMs just as observed in the experiments. During the transition from type I to type II ELMs, both types of ELMs are observed. In this state, some of the intermediate-n modes can destabilize the low-n modes, but not all. As the plasma becomes more and more stable against the low-n modes, fewer and fewer intermediate-n modes can lead to a wide low-n instability. The type I ELMs become less and less frequent until they are completely replaced by the smaller type II ELMs.

In the peeling–ballooning mode stability analysis, we investigated mode numbers up to $n = 8$ because the run times of the stability code become excessive in thorough analysis of higher mode numbers. A few sample cases with $n = 15$ showed similar mode structure with $n = 8$ with even narrower mode width and higher growth rate. Furthermore, in this analysis, the plasma was assumed static without any flows. Future investigations should consider higher mode numbers and possible effects of sheared flows on the stability.

Acknowledgments

We would like to thank T. Kurki-Suonio for useful discussions. This work was supported in part by EURATOM Mobility scheme.

References

[1] Leonard A.W. *et al* 1999 *J. Nucl. Mater.* **266–269** 109
[2] Connor J.W. 1998 *Plasma Phys. Control. Fusion* **40** 191
[3] Connor J.W. *et al* 1998 *Phys. Plasmas* **5** 2687
[4] Snyder P.B. *et al* 2002 *Phys. Plasmas* **9** 2037
[5] Saarelma S. *et al* 2000 *Plasma Phys. Control. Fusion* **42** A139
[6] Stober J. *et al* 2001 *Nucl. Fusion* **41** 1123
[7] Sauter O. *et al* 1999 *Phys. Plasmas* **6** 2834
[8] Kamada Y. *et al* 2000 *Plasma Phys. Control. Fusion* **42** A247
[9] Bernard L.C. *et al* 1981 *Comp. Phys. Comm.* **24** 377
[10] Maraschek M. *et al* 1998 *Proc. 25th European Physical Society Conf. on Controlled Fusion and Plasma Physics, Prague (European Physical Society)* p 492
[11] Lao L.L. *et al* 2001 *Nucl. Fusion* **41** 295
[12] Saibene G. *et al* 2002 *Plasma Phys. Control. Fusion* **44** 1769
[13] Kurita G. *et al* 1999 *Plasma Phys. Control. Fusion* **41** 159
[14] Ryter F. *et al* 2001 *Nucl. Fusion* **41** 537